PRINCIPLES OF OPERATION AND PERFORMANCE ESTIMATION OF CENTRIFUGAL COMPRESSORS

by

Dr. Meherwan P. Boyce

Chairman and CEO

Boyce Engineering International, Inc.

Houston, Texas

Meherwan P. Boyce is Chairman and CEO of Boyce Engineering International, Inc., in Houston, Texas. His past experience incorporates many academic and professional positions, including Professor of Mechanical Engineering, Founder and first Director of the Turbomachinery Laboratory. He was also responsible for founding the Turbomachinery Symposium, which he chaired for eight years.

His industrial positions include Manager of Compressor and Turbine development at Curtiss Wright and Manager of Aerodynamics Technology at Fairchild Hiller Corporation.

Dr. Boyce has written more than 100 significant publications and technical reports and is the author of the Gas Turbine Engineering Handbook *and has contributed to other major handbooks. He has been elected to membership in several honor societies such as Phi Kappa Phi, Pi Tau Sigma, Sigma Xi, and Tau Beta Pi.*

He is also a member of several professional socities such as ASME, SAE, NSPE, HESS and ASEE. In 1985, Dr. Boyce was named an ASME Fellow. Dr. Boyce was the 1974 recipient of the ASME Herbert Allen Award for Excellence and the 1973 recipient of the Ralph R. Teetor Award of SAE.

Dr. Boyce pioneered a breakthrough in technology through the development of a real time computer system which monitors, analyzes, diagnoses, and prognisticates performance of major turbomachinery. These systems are in use throughout the world.

Dr. Boyce received his Ph.D. in Mechanical Engineering from the University of Oklahoma.

INTRODUCTION

A compressor is a fluid handling mechanical device capable of efficiently transferring energy to the fluid medium so that it can be delivered in large quantities at elevated pressure conditions. Compressors have numerous applications ranging from aircraft and process industries to household appliances such as refrigerators and air conditioners. There are numerous types of compressors, each suitable for a particular application. Generally, compressors can be categorized under two basic types—positive displacement and dynamic. Positive displacement compressors include piston, screw, vane, and lobe compressors. Axial and centrifugal compressor types are dynamic compressors as the required pressure rise and flow is imparted to the fluid medium by transferring kinetic energy to the process gas.

Flowrate, efficiency, and the pressure rise within the compressor are the three most important parameters used in defining the performance of a compressor and in its selection. Typical performance characteristics are shown in Figure 1 of different types of compressors.

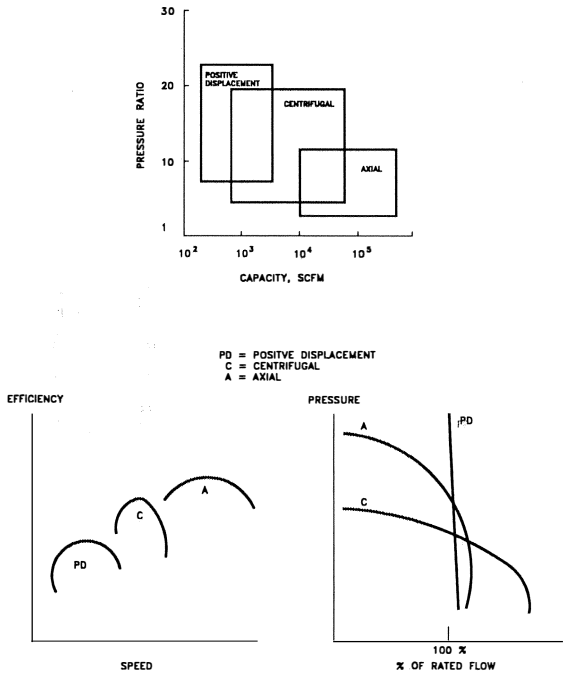

Figure 1. Performance Characteristics of Various Types of Compressors.

Positive displacement compressors are generally suitable for small flowrates while centrifugal and axial compressors are more commonly applied for medium and large flow applications respectively. The advantages of centrifugal compressors are that they are reliable, compact and robust, have better resistance to foreign object damage, and are less affected by performance degradation due to fouling. Above all, as can be seen in Figure 1, they have a wider operating domain when compared to other compressor types.

Centrifugal compressors are most commonly applied in petrochemical or process industries in the flowrates ranging from 1000 to 100,000 ft^3/min. Typical centrifugal compressor applications are summarized in Table 1.

BASIC COMPONENTS AND PRINCIPLES OF OPERATION

A centrifugal compressor (Figure 2) consists of three basic parts: (1) rotor assembly (impeller), (2) diffuser, and (3) scroll. Inlet guide vanes direct the flow to the inducer at the right rotor

Table 1. Application of Centrifugal Compressors

Industry or Application	Service of Process	Typical Gas Handled
Iron and Steel		
Blast furnace	Combustion	Air
	Off Gas	Blast furnace gas
Bessemer converter	Oxidation	Air
Cupola	Combustion	Air
Coke oven	Compressing	Coke oven gas
	exhausting	Coke oven gas
Mining and Metallurgy		
Power	For tools and machinery	Air
Furnaces	Copper and nickel purification	Air
	Pelletizing (Iron Ore concentration)	Air
Natural Gas		
Production	Repressuring oil wells	Natural gas
Distribution	Transmission	Natural gas
Processing	Natural gasoline separation	Natural gas
	Refrigeration	Propane and Methane
Refrigeration		
Chemical	Various Processes	Butane, propane, ethylene, ammonia, special refrigerants
Industrial and commercial	Air conditioning	Special refrigerants

inlet angle. The rotor increases kinetic energy of the medium as well as its static and total pressure (Figure 3).

Total conditions only vary when energy is put into the system, thus only in the impeller. The gas leaves the rotor and enters the diffuser at an angle determined by the rotor exit angle and the rotational speed of the rotor. The primary purpose of the diffuser

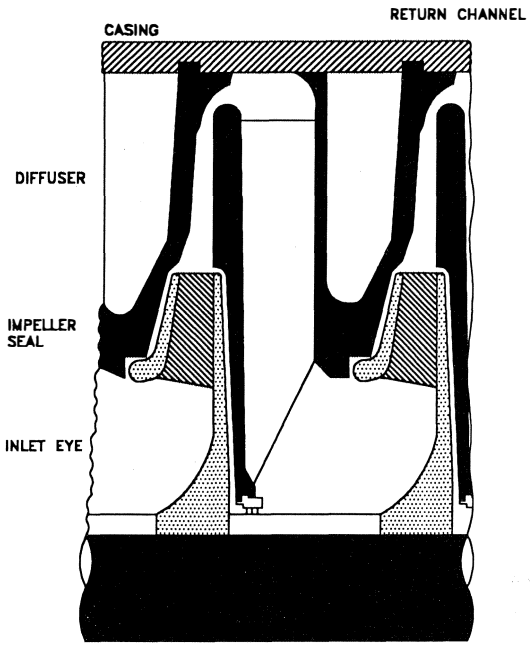

Figure 2. Schematic of Centrifugal Compressor.

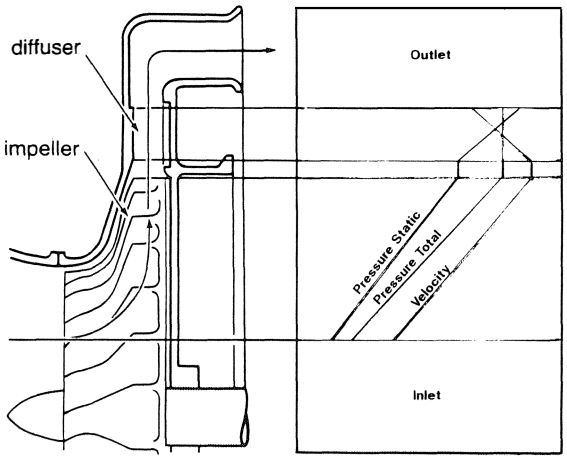

Figure 3. Variation of Pressure and Velocity through the Compressor.

is to reduce the velocity of the gas and to efficiently increase the static pressure. In the case of the centrifugal compressor, since the flow direction is in the radially outward direction, the increase in flow area in the downstream direction naturally diffuses the flow. The compressed gas from the diffuser discharges into the rotor downstream through return bend and return channel. The last diffuser discharges the gas to a scroll or volute. The cross-section of the scroll varies circumferentially. Since all the rotating blade passages discharge the compressed gas into the scroll, the cross-section of the scroll increases in the direction of rotation of the rotor. The increase in scroll cross-section is also designed to give additional pressure rise. Since the gaseous medium passes though a labyrinth of rotating and stationary flow passages, the entire gas path has to be aerodynamically designed to compress the gas efficiently and minimize losses.

DIMENSIONAL ANALYSIS OF A CENTRIFUGAL COMPRESSOR

Turbomachines can be compared with each other by the use of dimensional analysis. This type of analysis produces various types of geometrically similar parameters. Dimensional analysis is a procedure where variables representing a physical situation are reduced into groups that are dimensionless. These dimensionless groups can then be used to compare performance of various types of machines with each other. Dimensional analysis as used in turbomachines can be used for the following: (1) to compare data from various types of machines, (2) a very useful technique in the development of blade passages, blade profiles, and diffusers for selection of various types of units based on maximum efficiency and pressure head required, and 3) prediction of a prototype units performance from test conducted on a smaller scale model or at lower speeds and flows. Some of the important nondimensional parameters are:

$$\text{Reynolds number} \quad Re = \frac{\rho D V}{\mu} \tag{1}$$

$$\text{Specific Speed} \quad N_s = \frac{N\sqrt{Q}}{H^{3/4}} \tag{2}$$

$$\text{Specific Diameter} \quad D_s = \frac{DH^{3/4}}{\sqrt{Q}} \tag{3}$$

$$\text{Flow Coefficient} \quad \Phi = \frac{H}{ND^3} \tag{4}$$

$$\text{Head Coefficient} \quad \Psi = \frac{H}{N^2D^2} \tag{5}$$

where D, H, V, N are, respectively, diameter of the impeller, head, velocity, and speed of the machine. The aforementioned are some of the major dimensionless parameters. In many cases, for the flow to remain dynamically similar, all the above parameters must remain constant; however, this is not possible in a practical sense, so one must make choices.

In selecting turbomachines, the choice of specific speed and specific diameter determines the type of compressor which is most suitable as seen in Figure 4

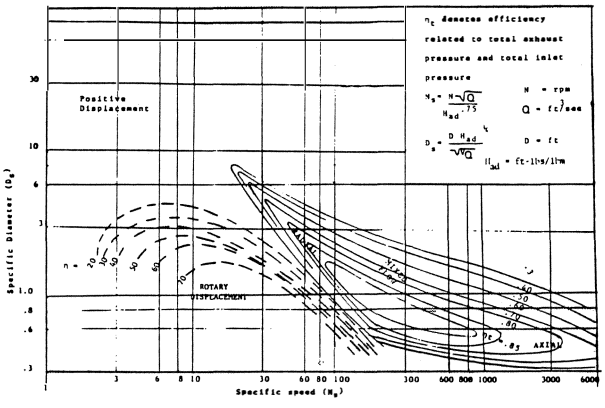

Figure 4. A Generalized Compressor Map.

It is obvious from this figure that high head and low flow require a positive displacement type unit, while a medium head and medium flow require a centrifugal type unit, and for high flow and low head an axial flow type compressor is the best choice.

A detailed view is shown in Figure 5 of the centrifugal compressor section of Figure 4 and can be used as a reference for selection of centrifugal compressor units. Flow coefficients and pressure coefficients can be used to determine various off design characteristics. The Reynolds number affects the flow calculations as far as the skin friction and velocity distribution are concerned. It must be remembered when using dimensional analysis in computing performance or predicting performance based on tests performed on smaller scale units that, due to the fact that it is not physically possible to keep all parameters constant, the variation of the final results will depend on the scale up factor, the difference in the fluid medium, the speed of the unit, and the pressure delivery. It is therefore very important to understand the limit of the parameters and thus the geometrical scale up while conducting a dimensional study.

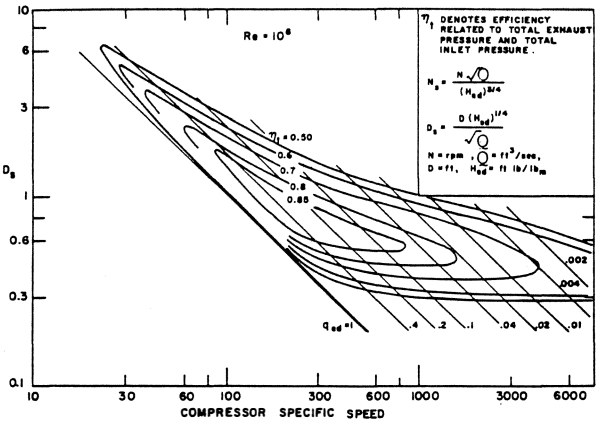

Figure 5. A Typical Centrifugal Compressor Performance Chart.

Basic Equations

Euler Turbine Equation

The Euler equation is a modification of the mathematical formulation of the law of conservation of momentum. It states that the rate of change in linear momentum of a volume moving with the fluid is equal to the surface forces and body forces acting on the fluid. The velocity components in a generalized turbomachine are shown in Figure 6. The velocity vectors as shown are resolved into three mutually perpendicular components: the axial component (V_z), the tangential component (V) and the radial component (V_r).

By examining each of these velocities, the following characteristics can be noted: the change in the magnitude of the axial velocity gives rise to an axial force that is countered by a thrust bearing and the change in radial velocity gives rise to a radial force that is countered by the journal bearing. The tangential component is the only component that causes a force which corresponds to a change in angular momentum; the other two velocity components have no effect on this force—except for what bearing friction may arise. By applying the conservation of momentum principle, the change in angular momentum obtained by the change in the tangential velocity is equal to the summation of all the forces applied on the rotor. This summation is the net torque of the rotor.

A certain mass of fluid enters the turbomachine with an initial velocity (V_1) at a radius r_1, and leaves with a tangential velocity (V_2) at a radius r_2. Assuming that the mass flowrate through the turbomachine remains unchanged, the torque exerted by the change in angular velocity can be written as:

$$\tau = \frac{\dot{m}}{g_c}(r_1 V_{\theta 1} - r_2 V_{\theta 2}) \tag{6}$$

The rate of change of energy transfer ft-lb_f/sec is the product of the torque and the angular velocity

$$\tau\omega = \frac{\dot{m}}{g_c}(r_1 V_{\theta 1} - r_2 \omega V_{\theta 2}) \tag{7}$$

Thus, the total energy transfer is given by the following relationship:

$$E = \frac{\dot{m}}{g_c}(U_1 V_{\theta 1} - U_2 V_{\theta 2}) \tag{8}$$

where U_1 and U_2 are the linear velocity of the rotor at the respective radii and (V_1) and (V_2) are the tangential projections of the absolute velocity. The previous relation for unit mass flow can be reduced to the following:

$$H = \frac{1}{g_c}(U_1 V_{\theta 1} - U_2 V_{\theta 2}) \tag{9}$$

where H is the energy transfer per unit mass flow ft-lb_f/lb_m, commonly known as the head, is delivered. Understanding the basics of this equation helps in visualizing practical turbomachinery operation.

As simple as it seems, this equation is the basis of nearly all performance characteristics in turbomachines.

Based on the energy equation and using measured variables, the specific work and head can be evaluated as:

$$H = h_2 - h_1 \cong C_p(T_2 - T_1) = \frac{C_p T_1}{\eta}\left[\left(\frac{P_2}{P_1}\right)^{\frac{\gamma-1}{\gamma}} - 1\right] \tag{10}$$

where h_2 and h_1 are inlet and exit gas enthalpies that are direct functions of compressor inlet and exit temperatures and pressures. For a thermally and callorically perfect gas, specific enthalpy is a

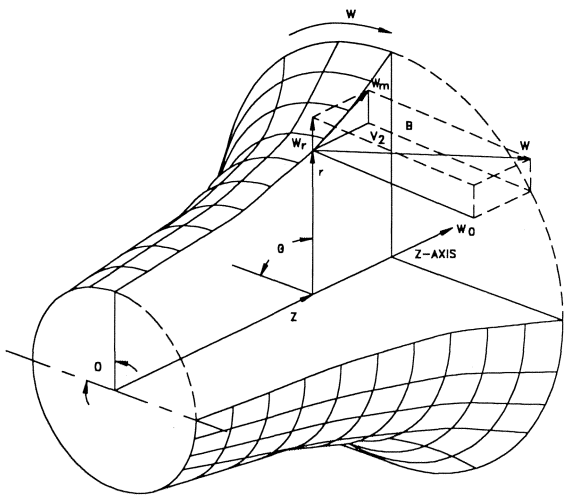

Figure 6. Velocity Vectors in Compressor Rotor Flow.

product of specific heat at constant pressure (C_p) and temperature, as shown in Equation 10.

The only difference between the above equations is that while Equation (9) is based on mechanical principles, Equation (10) is based on thermal quantities and can be explained clearly in terms of the first law of thermodynamics that heat and work are interchangeable. These two equations can be equated using the definition of efficiency. While Equation (9) is used to design a turbomachine, Equation (10) is useful to quantify the efficiency of the design. Equations (9) and (10) can be combined together to relate the running conditions and the compressor impeller geometry to the pressure rise within the compressor as:

$$\frac{P_2}{P_1} = \left[1 + \frac{n}{C_p T_2 g_c}\,(U_2 V_{\theta 2} - U_1 V_{\theta 1})\right]^{\frac{\gamma - 1}{\gamma}} \qquad (11)$$

The compressor performance is thus clearly interrelated to the compressor geometry.

Energy Transformation in Turbomachines

The compressor rotor transfers its kinetic energy to the gas within the impeller. However, not all the energy of the gas gets converted into pressure (potential) energy within the impeller. As explained in the introduction, the diffuser and volute or scroll aid in transferring energy of high velocity gases into pressure. The distribution of energy transfer within the compressor is dictated by its design. Using basic trigonometry Equation (11) can be rewritten as:

$$H = \frac{1}{2g_c}\left[(V_2^2 - V_1^2) + (U_2^2 - U_1^2) + (W_1^2 - W_2^2)\right] \qquad (12)$$

The first term in the above equation, $1/2g_c\,(V_2^2 - V_1^2)$, termed the *external effect* represents the kinetic energy transferred to the gas from the rotor. This term represents the virtual pressure rise possible external to the rotor but within the compressor using the diffuser and scroll. The second term, $1/2g_c\,(U_2^2 - U_1^2)$, describes the pressure rise possible within the rotor due to the *centrifugal effect* which is only possible in centrifugal compressors or radial inflow turbines where the rotor entrance and exit are at different radii. The third term, $1/2g_c(W_2^2 - W_1^2)$, represents the *internal diffusion effect* describing the pressure rise possible within the rotor, by reducing the relative velocity within the rotor. Clearly, since a centrifugal compressor takes advantage of the *centrifugal effect*, it can produce a higher pressure rise per stage than an axial compressor. Also, the crosssectional area variation of the flow passage (between the vanes) and the rotor inlet and exit flow angles are critical to determine the work distribution among the rotor, diffuser, and scroll in compressing the gas.

COMPRESSOR PERFORMANCE

Compressor performance curves consists primarily of a plot showing the variation of compressor head or pressure ratio and efficiency at various constant rpm conditions at different mass flowrates such as the one shown in Figure 7. It can be seen from Figure 7 that an increase in rotor speed increases the compressor flowrate. At a particular rotor speed an increase in compressor pressure ratio can be obtained by reducing the compressor mass flowrate. This is to be expected because an increase in pressure at compressor delivery can only be expected if there is a *resistance* to flow, otherwise, the compressor would behave more like a fan or a blower. In a similar fashion, an increase in flowrate at constant rpm can be obtained by a reduction in the resistance at the compressor exit. An enhancement of compressor flowrate at *constant delivery pressure* is also possible. This requirement, however, can be met by not only changing exit throttle, but also increasing the compressor rpm. Minimum and maximum permissible flowrates at constant rpm are termed surge and choke limits. A line tracing the stall points of all the constant rpm lines is called a *surge line*. Similarly, locus of operating points of the compressor at various rpm is termed operating line. The compressor rotor should be designed such that at constant rpm, its efficiency peaks close to the surge line, as is indicated in Figure 7, that is, when the compressor pressure ratio is maximum.

Compressor Efficiencies

The work in a compressor under ideal conditions occurs at constant entropy as shown in Figure 8. The actual work done is indicated by the dotted line. The isentropic efficiency of the compressor can be written in terms of the total changes in enthalpy.

$$\eta_{ad_c} = \frac{\text{Isentropic Work}}{\text{Actual}} = \frac{(h_{2t} - h_{1t})id}{(h_{2't} - h_{1t})act} \qquad (13)$$

This equation can be rewritten for a thermally and calorifically perfect gas in terms of total pressure and temperature as follows:

$$\eta_{ad_c} = \left[\left(\frac{P_{2t}}{P_{1t}}\right)^{\frac{\gamma - 1}{\gamma}} - 1\right] \Big/ \left[\frac{T_{2t}}{T_{1t}} - 1\right] \qquad (14)$$

The process between 1 and 2′ can be defined by the following equation of state:

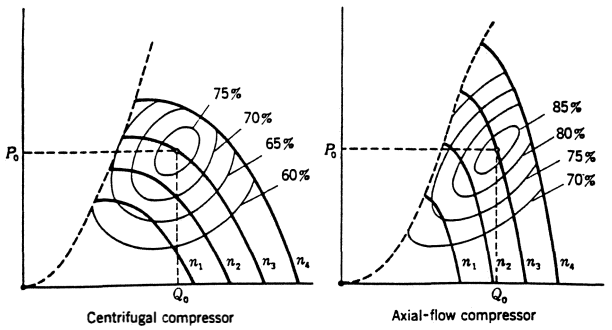

Figure 7. Compressor Performance Curves.

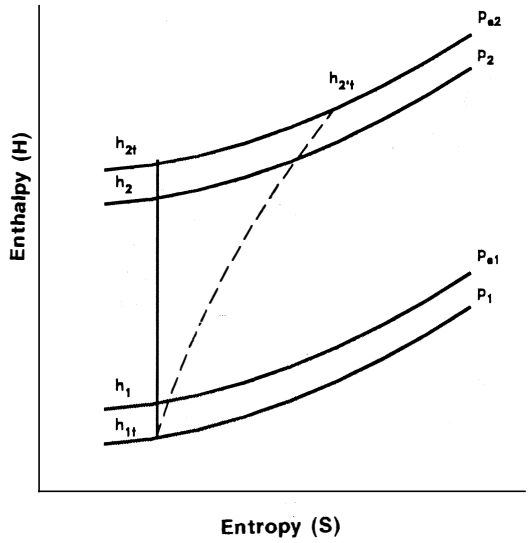

Figure 8. Temperature Entropy Diagram of a Compressor.

$$\frac{P}{\rho^n} = \text{Const} \tag{15}$$

Where η is some polytropic process. The adiabatic efficiency can then be represented by:

$$\eta_{ad_c} = \left[\left(\frac{P_{2t}}{P_{1t}}\right)^{\frac{\gamma-1}{\gamma}} - 1\right] \Big/ \left[\left(\frac{P_{2t}}{P_{1t}}\right)^{\frac{n-1}{n}} - 1\right] \tag{16}$$

Polytropic Efficiency

Polytropic efficiency is another concept of efficiency often used in compressor evaluation. It is often referred to as small stage or infinitesimal stage efficiency. It is the true aerodynamic efficiency exclusive of the pressure-ratio effect. The efficiency is the same as if the fluid is incompressible and identical with the hydraulic efficiency:

$$\eta_{\rho c} = \frac{\left[1 + \frac{dP_{2t}}{P_{1t}}\right]^{\frac{\gamma-1}{\gamma}} - 1}{\left[1 + \frac{dP_{2t}}{P_{1t}}\right]^{\frac{n-1}{n}} - 1} \tag{17}$$

which can be expanded assuming that

$$\frac{dP_{2t}}{P_{1t}} << 1 \tag{18}$$

Neglecting second order terms, the following relationship is obtained:

$$\eta_{\rho c} = \frac{\frac{\gamma-1}{\gamma}}{\frac{n-1}{n}} \tag{19}$$

From this relationship, it is obvious that polytropic efficiency is the limiting value of the isentropic efficiency as the pressure increases approaches zero, and the value of the polytropic efficiency is higher than the corresponding adiabatic efficiency. The relationship between adiabatic and polytropic efficiency is shown in Figure 9, as the pressure ratio across the compressor increases. Another characteristic of polytropic efficiency is that the polytropic efficiency of a multistage unit is equal to the stage efficiency, if each stage has the same efficiency.

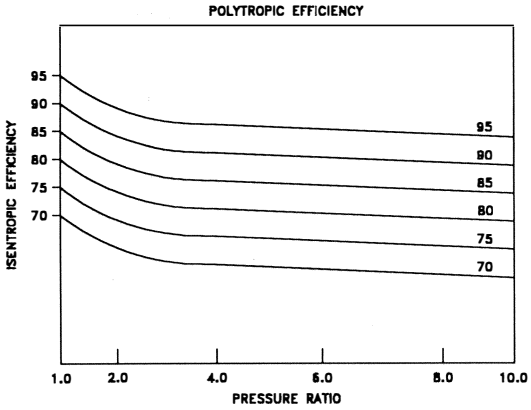

Figure 9. Relationship between Adiabatic and Polytropic Efficiency Compressor.

Factors Affecting Compressor Performance

A number of factors can affect the compressor performance and these are described briefly in the following paragraphs.

Gas Composition

The performance characteristics of a compressor are not a function of compressor geometry alone, but also depend on the properties of the gas it is compressing.

Utilizing real gas effects ($PV = ZRT = A\ \frac{K}{MW}\ T$) where, Z is the compressibility factor, and $C_p = \frac{\gamma}{\gamma - 1}\ \frac{K}{MW}$, specific work or adiabatic head required to compress the gas is given by:

$$W = Z\ \frac{K}{MW}\ T_1\ \frac{\gamma}{\gamma - 1}\ \left(\frac{P_2}{P_1}^{\frac{\gamma-1}{\gamma}} - 1\right) \tag{20}$$

The specific work or energy required to compress the gas is a function of compressibility of the gaseous mixture, the equivalent mixture molecular weight, and the inlet and exit pressure conditions, as indicated in Equation (20). Hence, if the molecular weight of the gas increases, for the same specific work, the pressure ratio of the compressor also increases. Also, the mass flowrate increases proportional to the molecular weight of the gas, volume flowrate on the other hand remains constant.

The performance is shown in Figure 10 of an individual stage at a given speed for three level of gas molecular weight. The heavy gas class includes gases such as propane, propylene and standardized refrigerant mixtures. Air, natural gases and nitrogen are typical of the medium class gases. Hydrogen rich gases found in hydrocarbon processing plants are representative of the light class gases.

The following observations can be made with respect to the curve for heavy gas as compared to lighter gas.

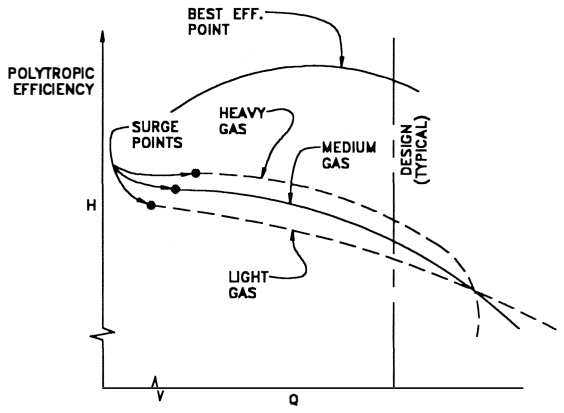

Figure 10. Effect of Performance of Various Gases.

- The flow at surge is higher.
- The stage produces more head than that corresponding to medium or lighter gas.
- The right hand side of the curve near choke turns downward (approaches stonewall) more rapidly.
- The curve is flatter towards the surge point.

Inlet Conditions

Specific head developed by the compressor given in Equation (12) is the amount of energy transferred by the rotor to the gas and, hence, is a function of rotor speed and geometry only and is not affected by inlet conditions. Using Equation (10), however, one can get an idea of variation in pressure ratio and power with ambient temperature variation.

Inlet Guide Vanes

The inlet guide vanes give a circumferential velocity component to the fluid at the inducer inlet. This is called prewhirl. The inducer inlet velocity diagrams are shown in Figure 11 with and without inlet guide vanes (IGV), which may be installed directly in front the inducer, or where an axial entry is not possible, located radially in an intake duct. A positive vane angle produces prewhirl in the direction of the impeller rotation and a negative vane angle produces prewhirl in the opposite direction. The disadvantage of positive prewhirl is that a positive inlet whirl velocity reduces the energy transfer. The Euler equation is defined by :

$$H = \frac{1}{g_c}(U_1 V_{\theta 1} - U_2 V_{\theta 2}) \qquad (21)$$

For non-prewhirl (without IGV) V_{el} is equal to zero. The Euler work is thus equal to $H = U_2 V_{el}2$. Euler work is reduced by the amount $U_1 V_{el}1$. in the case of positive prewhirl. Negative prewhirl increases the energy transfer by the amount $U_1 V_{el}1$. The positive prewhirl, on the other hand, decreases the relative mach number at the inducer inlet. This decrease in the relative Mach number is important for units operating at or near Mach numbers of 0.7. Negative prewhirl on the other hand increases the relative Mach number. A relative mach number is defined by:

$$M_{rel} = \frac{W_{rl}}{\alpha l} \qquad (22)$$

where: M_{rel} is the relative mach number, W_{rl} is the relative velocity at an inducer inlet and $\propto_1$ is the sonic velocity at an inducer inlet section based on the static temperature at that point.

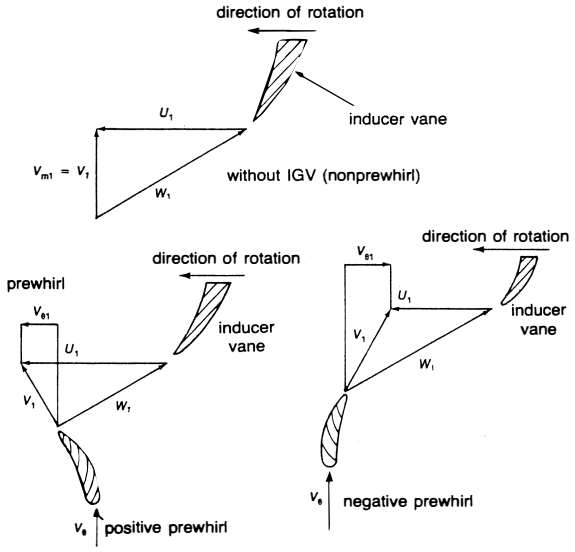

Figure 11. Inducer Inlet Velocity Diagram.

The main purpose, in most cases, of installing an IGV is to decrease the relative Mach number at the inducer tip inlet because the highest relative velocity occurs at the inducer inlet tip section. When the relative velocity is close to the sonic velocity or greater than it, a shock wave takes place at the inducer section, this gives the shock loss and also chokes the inducer. Relative mach numbers above 0.7 increase the losses dramatically. Negative pre swirl is rarely used since it also decreases the operating range. The effect of various guide vane settings on the ideal head of backward curved blades is shown in Figure 12. The effect of inlet prewhirl is shown in Figure 13 with respect to a compressor efficiency for high pressure radial bladed impellers.

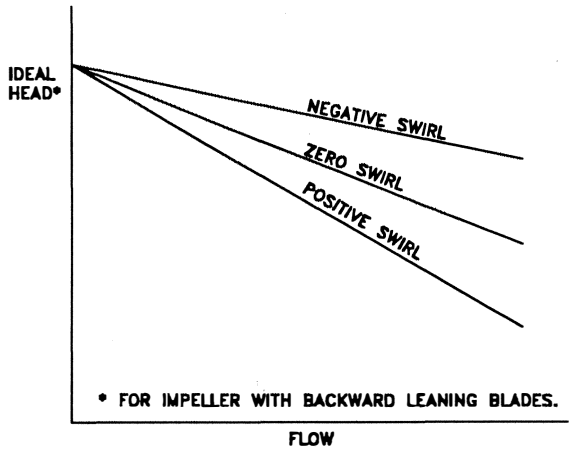

Figure 12. Swirl Effects on a Backward Curve Blade.

There are three kinds of prewhirl. These are as follows:

- *Free Vortex Type*—this type is represented by $r_1 V_1$ = constant with respect to the inducer inlet radius. This prewhirl distribution is shown in Figure 13. In this type, V_1 is a minimum at the inducer inlet shroud radius. Therefore, it is not good to decrease the relative Mach number in this manner.
- *Forced Vortex Type*—This type is shown as V_1/r_1 = constant, with respect to the inducer inlet radius. Prewhirl distribution with this type of inducer is shown in Figure 14. In this type, V_1 is a

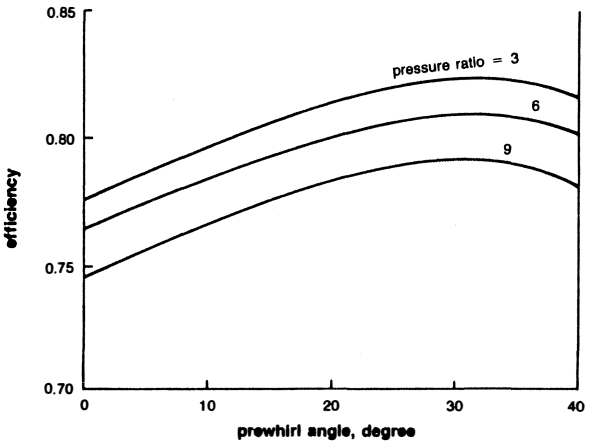

Figure 13. Effect of Prewhirl on Efficiency of High Pressure Compressor.

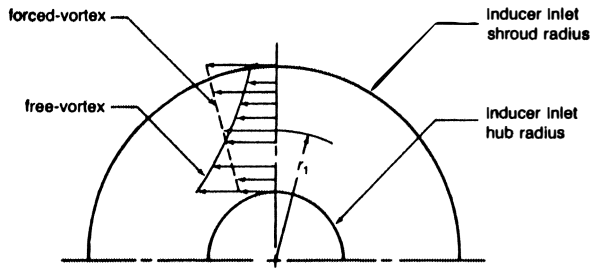

Figure 14. Prewhirl Distribution Patterns.

maximum at the inducer inlet shroud radius, so this contributes to decreasing the inlet relative Mach number.

• *Control Vortex Type*—This type is represented by $V_1 = Ar_1 + B/r_1$ where A and B are constants. This equation shows the first type with A = 0, B 0 and the second type with B = 0, A 0.

Euler work distributions at an impeller exit with respect to the impeller width are shown in Figure 15. From Figure 15, it is noted that the prewhirl distribution should be made not only from the relative Mach number at the inducer inlet shroud radius, but also from Euler work distribution at the impeller exit. This is because uniform impeller exit flow conditions, considering both the impeller and diffuser losses, are important factors to obtain good compressor performance.

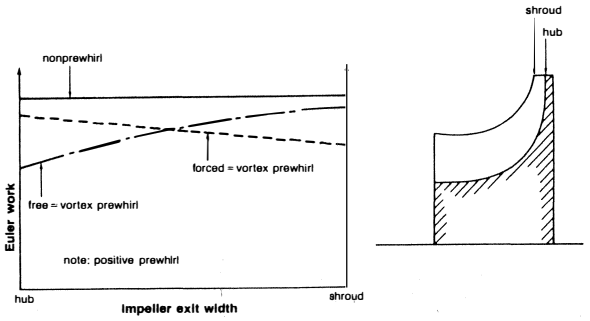

Figure 15. Euler Work Distribution at Impeller Exit.

Inducer

The function of an inducer is to increase the fluid's angular momentum without increasing its radius of rotation. In an inducer section, the blades bend toward the direction of rotation as shown in Figure 16. The inducer is an axial rotor and changes the flow direction from the inlet flow angle to the axial direction. It has the largest relative velocity in the impeller and, if not properly designed, can lead to choking conditions at its throat, as shown in Figure 16.

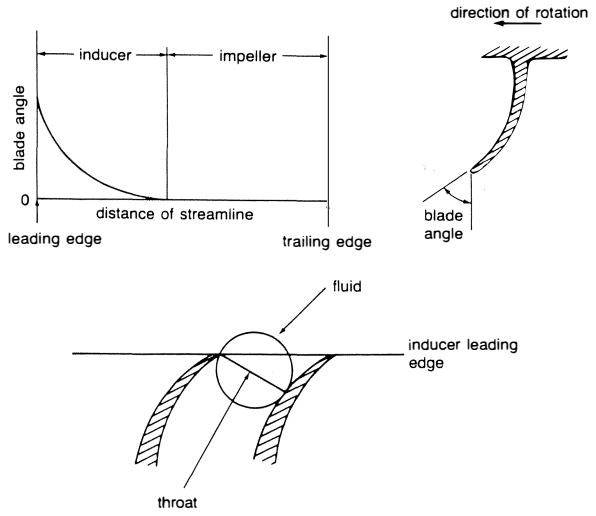

Figure 16. Inducer Centrifugal Compressor.

There are three forms of inducer camber lines in the axial direction. These are circular arc, parabolic arc, and elliptical arc. Circular arc camber lines are used in compressors with low pressure ratios, while the elliptical arc produces good performance at high pressure ratios where the flow has transonic mach numbers.

Because of choking conditions in the inducer, many compressors incorporate a splitter-blade design The flow pattern in such an inducer section is shown in Figure 17 (a). This flow pattern indicates a separation on the suction. Other designs include tandem inducers. In tandem inducers the inducer section is slightly rotated as shown in Figure 17 (b). This modification gives additional kinetic energy to the boundary layer, which is otherwise likely to separate.

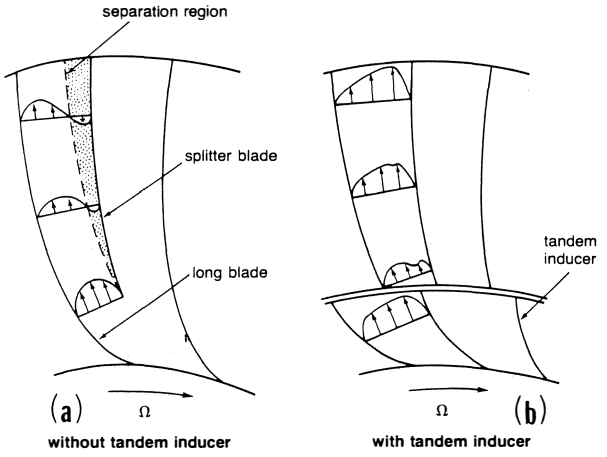

Figure 17. Impeller Channel Flow with a Splitter and Tandem Inducer.

Effect of Blade Shape On Performance

The blade shapes of centrifugal compressors can be classified based on rotor exit blade shape as backward, radial and forward curved blades, as shown in Figure 18. In order to study the effect of blade shape on performance one resorts to velocity triangles. The axial component of velocity represents the velocity vector proportional to the volume flowrate. To begin with, the flowrate and the head produced for the three blade shapes are assumed to be the same. By changing the volume flowrate for each of the three blade shapes, that is, by increasing the axial velocity vector for the three machines by the same amount one can determine the head produced from each of the blade shapes considered using the Euler Turbine equation. This exercise results in a plot as shown in Figure 19. Solid lines indicate ideal characteristics and dotted lines real characteristics which take losses into account. The figure clearly illustrates that in theory as the flowrate increases the head or pressure ratio of the compressor drops for backward-curved blades, remains almost the same for radial exit compressors and increases for forward-curved blades. Most impellers in the petrochemical field are radial or backward curved.

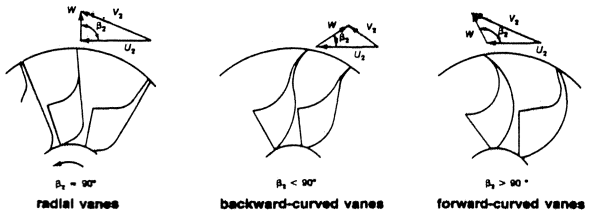

Figure 18. Velocity Triangles of Various Types of Impeller Blading.

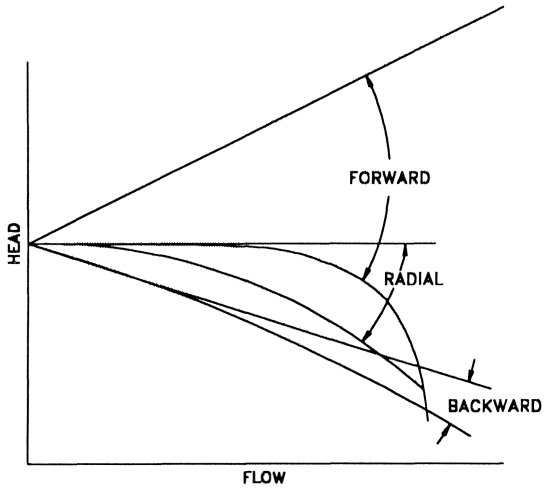

Figure 19. Head and Flowrate Characteristics of Various Impeller Blading.

Slip

The high velocity exiting from the forward bladed impeller increases the losses in the diffuser section decreasing the efficiency in such a compressor to unacceptable levels. Blades should be designed to eliminate large decelerations or accelerations of flow in the impeller that lead to high losses and separation of the flow. The velocity distributions measured in a typical centrifugal compressor are shown in Figure 20.

In the previous section, the performance characteristics of three types of rotors were introduced. These are radial, backward, and

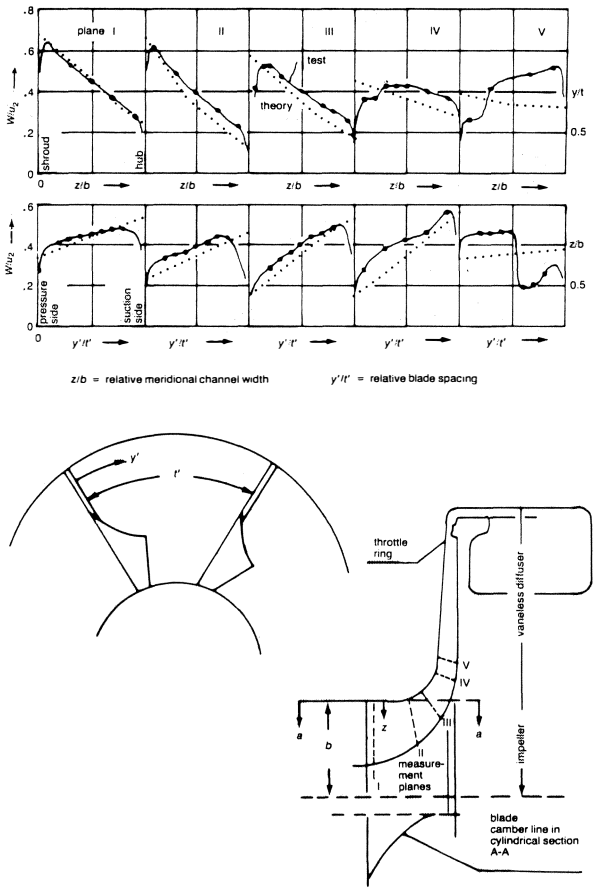

Figure 20. Velocity Profiles Through a Centrifugal Impeller.

forward curved blades at the rotor exit. The relative velocity of the gas leaving the rotor does not exactly follow the exit rotor angle. This phenomenon is due to circulation or slip which occurs in various blade compartments. The effect of slip on the exit flow angle is illustrated in Figure 21.

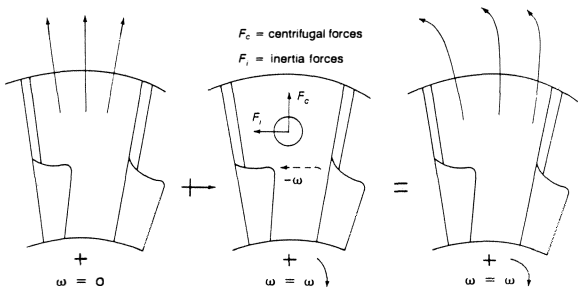

Figure 21. Forces and Flow Characteristics in a Centrifugal Impeller.

To account for the flow deviation (which is similar to the effect accounted for by the deviation angle in axial flow machines), a factor known as the slip factor is used, defined as, $=V_{\theta 2act}/V_{\theta 2th}$, where V_{e2act} is the tangential component of the absolute exit velocity and $V_{\theta 2th}$ is the theoretical component of the absolute exit velocity.

Causes of Slip

The cause of the slip factor phenomenon that occurs within an impeller is not known exactly. However, some general reasons can be used to explain why the flow is changed, these are:

• *Coriolis Circulation*—The pressure gradient between the walls of two adjacent blades, Coriolis force and centrifugal force causes circulation of the fluid within the rotor flow passages as shown in Figure 22. Because of this circulation, a velocity gradient results at the impeller exit with a net change in the exit angle.

• *Boundary layer Development*—The boundary layer that develops within an impeller passage causes the flowing fluid to experience a smaller exit area as shown in Figure 23. This is due to small, if any, flow within the boundary-layer. For the fluid to exit this smaller area, its velocity must increase. This gives a higher relative exit velocity. Since the meridional velocity remains constant, the increase in relative velocity must be accompanied with a decrease in absolute velocity.

• *Leakage*—Fluid flow from one side of a blade to the other side is referred to as leakage. Leakage reduces the energy transfer from impeller to fluid and decreases the exit velocity angle.

• *Number of Vanes*—The higher the number of vanes, the lower the vane loading and the closer the fluid follows the vanes. With higher vane loadings, the flow tends to group upon the pressure surfaces and introduces a velocity gradient at the exit.

• *Vane Thickness*—Due to manufacturing problems and physical necessity, impeller vanes have some thickness. When the fluid exits the impeller, the vanes no longer contain the flow and the meridional velocity is immediately decreased, both the relative and absolute velocities decrease, thus changing the exit angle of the fluid.

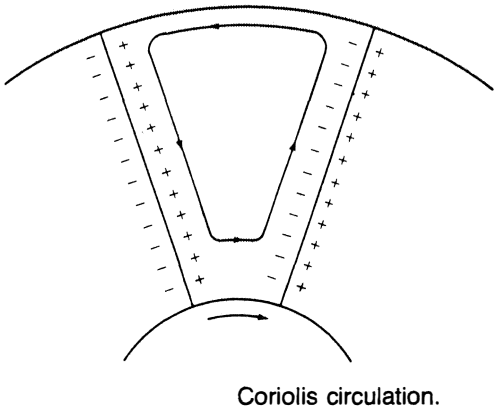

Figure 22. Coriolis Circulation in a Centrifugal Impeller.

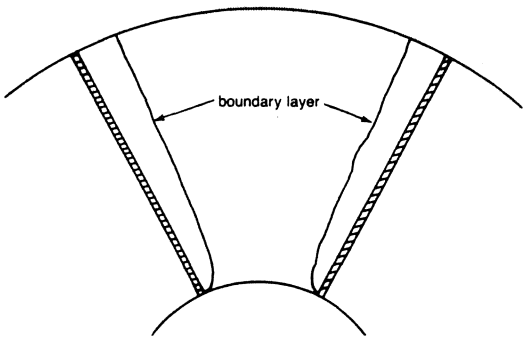

Figure 23. Boundary-Layer Development in a Centrifugal Impeller.

To combine all these effects, consider a backward curved blade impeller. The exit velocity triangle for this impeller, with the different slip phenomenon changes is shown in Figure 24. As this show the actual conditions when the compressor is running may be far removed from the design condition.

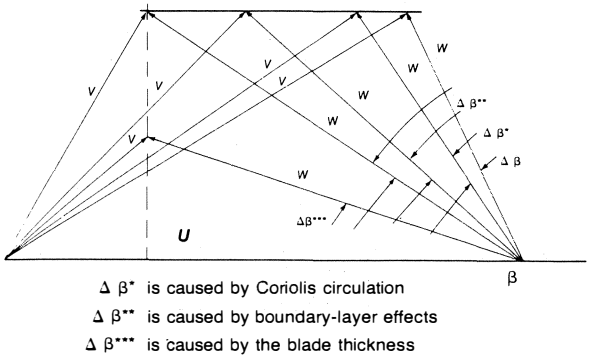

Figure 24. Effect on Exit Velocity Triangle by Various Parameters Which Cause Slip.

Several empirical equations have been derived for the slip factor. Some of the more widely used methods equations are derived by Stodola and Stanitz.

Slip Factor Due to Stodola

The second Helmholtz law states that the vorticity of a frictionless fluid does not change with time. Hence, if the flow at the inlet to an impeller is irrotational, the absolute flow must remain irrotational throughout the impeller. As the impeller has an angular velocity, the fluid must have an angular velocity, relative to the impeller. This fluid motion is called the relative eddy. Thus, if there were no flow through the impeller, the fluid in the impeller channels would rotate with an angular velocity equal and opposite to the impeller's angular velocity.

To approximate the flow, Stodola's theory assumes that the slip is due to the relative eddy. The relative eddy is considered as a rotation of a cylinder of fluid at the end of the blade passage (shown as a shaded circle) at an angular velocity of about its own axis. The Stodola slip factor is given by,

$$\mu = 1 - \frac{\pi}{Z}\left(1 - \frac{\sin\beta_2}{\frac{Wm_2 \cot\beta_2}{U_2}}\right) \qquad (23)$$

where β_2 is the blade angle, Z the number of blades, Wm_2 is the meridional velocity and U_2 the blade tip speed. Calculations using this equation have been found to be generally lower than experimental values.

Stantiz Slip Factor

Stanitz calculated blade-to-blade solutions for eight impellers and concluded that, for the range of conditions covered by the solutions, U is a function of the number of blades (Z) and the blade exit angle (β_2) is approximately the same whether the flow is compressible or incompressible.

$$\mu = 1 - \frac{0.63\pi}{Z}\left(1 - \frac{1}{\frac{Wm_2}{U_2}\cot\beta_2}\right) \qquad (24)$$

Stanitz's solutions were for $\pi/4<\beta_2<\pi/2$. This equation compares well with experimental results for radial or near radial blades.

Diffusers

Most centrifugal compressors in service in petroleum or petrochemical processing plants use vaneless diffusers. A vaneless diffuser is generally a simple flow channel with parallel walls and does not have any elements inside to guide the flow. The velocity diagrams shown in Figure 25 at the eye and exit of an impeller illustrate the trajectory a particle in the gas flow would take through a vaneless diffuser at the design condition (compressor rated point).

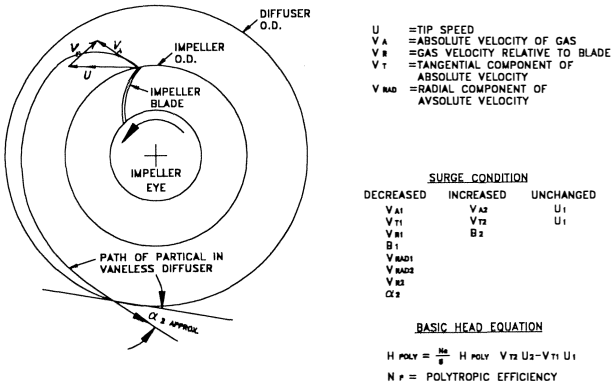

Figure 25. Surge Effect of Exit Velocity Diagrams.

When the inlet flow to the impeller is reduced while the speed is held constant, there is a decrease in V_{r2} and $\propto_2$. As $\propto_2$ decreases, the length of the flow path spiral increases. The effect is shown in Figure 26. If the flow path is extended enough, the flow momentum at the diffuser walls is excessively dissipated by friction and stall. With this greater loss, the diffuser becomes less efficient and converts a proportionately smaller part of the velocity head to pressure. As this condition progresses, the stage will eventually stall. This could lead to surge.

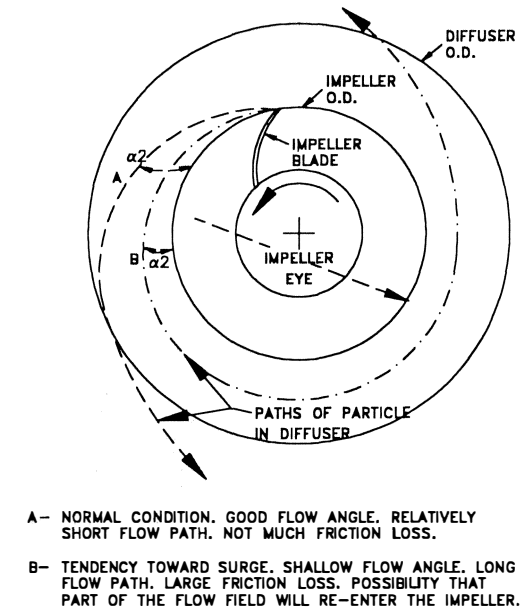

Figure 26. Flow Trajectory in a Vaneless Diffuser.

Vaned diffusers are used to force the flow to take a shorter, more efficient path through the diffuser. There are many styles of vaned diffusers, with major differences in the types of vanes, vane angles and contouring and vane spacing. Commonly used vane diffusers employ wedge-shaped vanes (vane islands) or thin curved vanes. The latter type of vane is illustrated in Figure 27. In high head stages, there can be two to four stages of diffusion. These usually are vaneless spaces to decelerate the flow, followed by two or three levels of vaned blades in order to prevent buildup of boundary layer, thus causing separation and surging the unit. The flow pattern in a vaned diffuser is indicated in Figure 27. The vaned diffuser can increase the efficiency of a stage by two to four percentage points, but the price for the efficiency gain is generally a narrower operating span on the head-flow curve with respect to both surge and stonewall. The effect of off-design flows is also shown in Figure 27. Excessive positive incidence at the leading edge of the diffuser vane occurs when $\propto_2$ is too small at reduced flow and this condition brings on stall. Conversely, as flow increases beyond the rated point, excessive negative incidence can cause stonewall. Despite its narrowing effect on the usable operating range on the characteristic curve, the vaned diffuser has its application in situations where efficiency is of utmost importance.

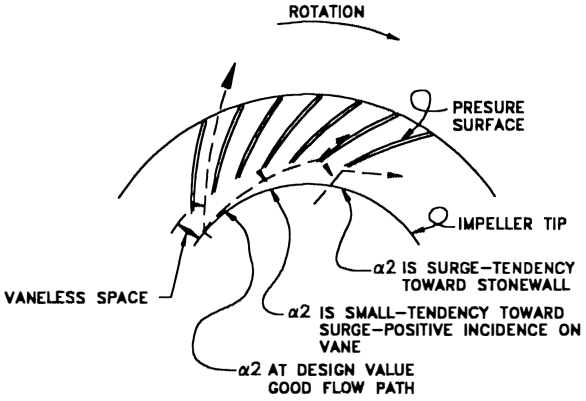

Figure 27. Flow Trajectory in a Vaned Diffuser.

Although seldom used, movable diffuser vanes or vane islands can be used to alleviate the shock losses at off-design conditions. However, as the adjusting mechanisms required are quite complicated, they generally are applied only to single-stage machines.

Losses in Centrifugal Compressors

Proper evaluation and estimation of centrifugal compressor performance requires knowledge of various types of losses within the compressor. Losses are typically expressed in terms of a reduction in total pressure. Losses are divided into two major groups—rotor and stator losses.

Rotor Losses

There are various types of rotor losses and are described briefly below.

• *Shock Loss*—This is common in compressors in aircraft applications and occur due to the presence of a compression shock wave at rotor inlet. Since a shock wave induces a ram pressure rise in a very small distance, it will be accompanied by a total pressure loss. Normal shock are accompanied by a greater pressure drop than an oblique shock. Hence, the compressor rotor inlet should be wedge-like, so as to obtain a weak oblique shock. If the blades were blunt, this would lead to a bow shock, which would cause the flow to detach from the blade leading edge and the loss to be much higher.

• *Incidence Loss*—At off design conditions, flow enters the inducer at an incidence angle that is either positive or negative. Fluid approaching a blade with incidence suffers an instantaneous change of velocity at the blade so as to comply with the blade inlet angle causing a total pressure loss. Incidence loss increases as the incidence angle increase.

• *Disk Friction Loss*—This is the loss due to the frictional torque on the back surface of the rotor between the hub and the casing. This loss is the same for a given size disk, whether it is used for a centrifugal compressor or a radial inflow turbine. In many cases, the losses in the seals, the bearings, and the gear box are also lumped in with this loss, and the entire loss can be called an external loss. In this loss, unless the gap is of the order of magnitude of the boundary layer, the effect of the gap size is negligible. A point of interest that should be indicated here is that the disk friction in a housing is less than that on a free disk. This is due the existence of a *core vortex* which rotates at half the angular velocity.

• *Diffusion Blading Loss*—This loss arises because of negative velocity gradients in the boundary layer. This deceleration of the flow increases the boundary layer and gives rise to a separation of the flow. The adverse pressure gradient, which a compressor normally works against, increases the chances of separation and gives rise to a rather significant loss.

• *Clearance Losses*—When a fluid particle has a translatory motion relative to a noninertial rotating coordinate system, it experiences, besides other forces, a force known as the coriolis force. A pressure difference exists between the driving and trailing faces of an impeller blade, due mainly to Coriolis acceleration. The shortest path, and generally that of least resistance, for the fluid to flow and neutralize this pressure differential, is provided by the clearance between the rotating impeller and the stationary casing. In the case of the shrouded impellers, such a leakage from the pressure side to the suction side of an impeller blade is not possible. Instead, the existence of a pressure gradient in the clearance between the casing and the impeller shrouds accounts for the clearance loss. Clearance loss may be substantial. The leak flow undergoes a large expansion and contraction due to temperature variation across the clearance gap affecting the leaking flow and the stream where it discharges.

• *Skin Friction Loss*—Skin friction loss is defined as the loss due to the shear forces on the impeller wall that are mostly due to turbulent friction. This type of loss is usually determined by considering the flow as an equivalent circular cross section with a hydraulic diameter. The loss is then computed based on the well known pipe flow pressure loss equations.

Stator Losses

• *Recirculating Loss*—This loss occurs due to the back flow into the impeller exit of compressor and is a direct function of the air exit angle. As the flow through the compressor reduces, at the same impeller speed, there is an increase in the absolute flow angle at the exit of the impeller. Loss results due to the mixing of direct and recirculating flow.

• *Wake Mixing Loss*—This loss is due to the mixing of the low velocity wake of the impeller blades with the main flow.

• *Vaneless Diffuser Loss*—This loss is the viscous flow loss experienced within the vaneless diffuser.

• *Vaned Diffuser Loss*—This takes into account the loss due to blade incidence angle and the skin friction due to the vanes. Vaned diffuser losses are based on the conical diffuser test results. They are a function of the impeller blade loading and the vaneless space radius ratio.

• *Exit Loss*—This loss is typically calculated by assuming that approximately one half of the kinetic energy leaving the vaned diffuser is lost.

Losses are complex phenomena and are a function of many parameters such as inlet conditions, pressure ratios, blade angles, flow, etc. The loss distribution is shown in Figure 28 in a typical and centrifugal stage of pressure ratio below 2:1 with backward curved blades.

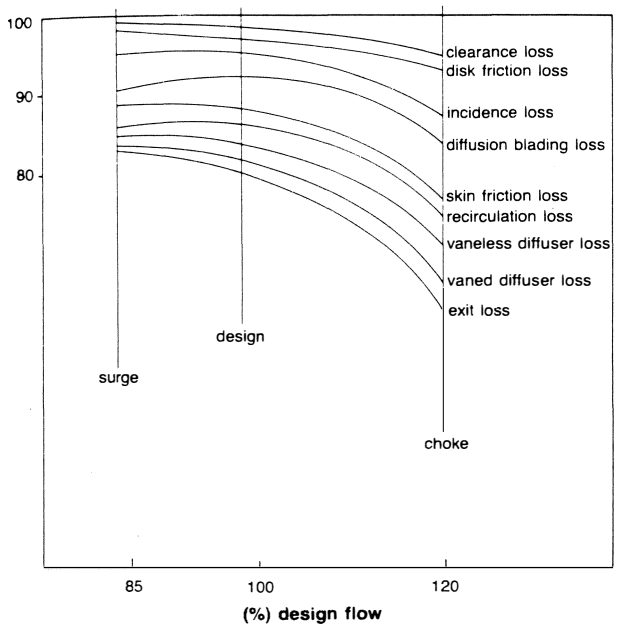

Figure 28. Losses in a Centrifugal Compressor.

COMPRESSOR SURGE

The phenomenon of surge, as it pertains to a centrifugal compressor and its connected systems, is an unstable condition resulting in flow reversals and pressure fluctuations in the system. This condition occurs when there is sufficient aerodynamic instability within the compressor that the compressor is unable to produce adequate pressure to deliver continuous flow to the downstream system. The system and compressor then interact causing the surge conditions with the large and sometimes violent flow oscillations in the system. Surge, then, is an overall system phenomenon and is not confined to the compressor only.

Surge is the result of an excessive increase in the resistance of the system while the compressor is operating at a certain speed. The added resistance reduces the flow to an unstable level. Alternatively, if the resistance is unchanged, but the speed is reduced appreciably, most systems will surge. Thus, surge occurrence depends on the type of system and the shape of the resistance curve.

The aerodynamic instability is brought about by flow reduction, which causes stalling of one or more of the elements of a stage or stages of the compressor. The stalling can occur at the inducer of the impeller, in the radial portion of the impeller, in the diffuser, or in the volute. A stall in one of these elements may not have sufficient effect to cause the stage to be unstable. In fact, several elements of a stage can stall without the entire stage stalling. However, if the stalling is of sufficient strength, the stage will become unstable, and this can lead to surge of the compressor.

A typical centrifugal multistage compressor performance map used in the process industry is shown in Figure 29. The family of

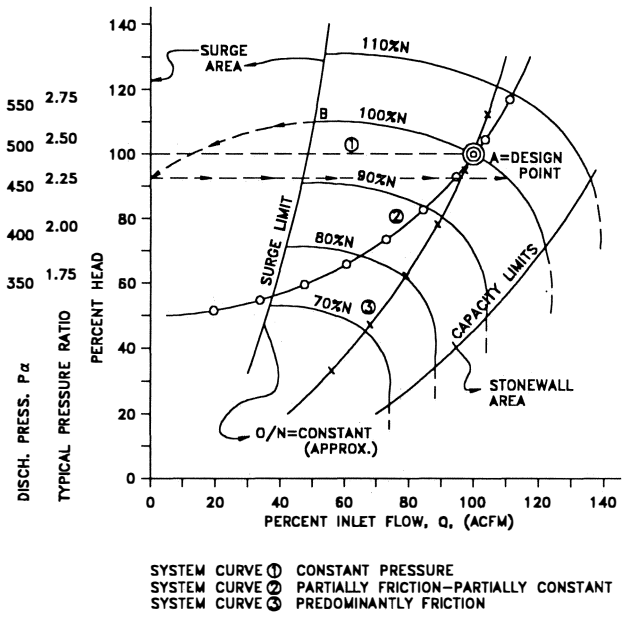

Figure 29. Performance Map with System Curves and Surge Cycles.

curves depicts the performance at various speeds, where N represents rpm. The ordinate may be head "H," pressure ratio, discharge pressure, or sometimes differential pressure. The abscissa, is shown usually always as the inlet flow. It is important to understand that the inlet flow volume or capacity is based on a gas with a particular molecular weight, specific heat ratio, and compressibility factor at a pressure and temperature corresponding to the gas condition in the suction line to the compressor. If any of these parameters is changed, the performance map is no longer exactly valid.

The line on the left represents the surge limit. Operation to the left of this line is unstable, resulting in unsatisfactory performance, and is often harmful mechanically. Notice that the surge flow increases as the speed increases. In many multistage units, and especially in units which are controlled by variable inlet guide vanes, the surge line curves bend dramatically at higher flows and speeds.

On the other side of the map, the capacity limit or overload line is shown. Operation to the right of this line causes the head-producing capability of the machine to fall off very rapidly, and the performance is difficult to predict. The area to the right of this line is commonly known as "choke" or "stonewall." Operating the machine in this region is usually harmless mechanically, although a few impeller failures have been ascribed to prolonged operation in stonewall.

The points labeled A, B, C, and D, and three typical system operating curves which have been plotted. The terms frequently used to define performance range is percent stability.

The rated "stable range" is generally taken as $Q_A - Q_B$, where Q_A is the design or rated point, and Q_B is the surge point along the 100% speed line. The percent stability is

$$\frac{Q_A - Q_B}{Q_A} \qquad (25)$$

expressed as a percentage.

The three representative system curves need little explanation. The shape of these curves is governed by the amount of friction, fixed pressure drop, or pressure control in the particular system external to the compressor through which the flow is being pumped. However, it should be noted that, to follow any one of these system curves, the speed must be changed. This, in turn, changes the flow. With Systems 2 and 3, the head is also changed. These statements are valid only if no changes within the system itself occur. Changing the setting of a control valve, adding another piping loop, or a changing catalyst level in a reactor which would modify the system curve.

To a large extent, the frequency of the surge cycle varies inversely with the volume of the system. For example, if the piping contains a check valve located near the compressor discharge nozzle, the frequency will be correspondingly much higher than that of a system with a large volume in the discharge upstream of a check valve. The frequency can be as low as a few cycles per minute or as high as 20 or more cycles per second. Generally speaking, if the frequency is higher, the intensity of surge is lower. The intensity or violence of surge tends to increase with increased gas density, which is directly related to higher molecular weights and pressures and lower temperatures. Higher differential pressure generally increases the intensity.

ROTATING STALL

Rotating stall (propagating stall) consists of large stall zones covering several blade passages, and propagates in the direction of the rotor and at some fraction of rotor speed. The number of stall zones and the propagating rates vary considerably. Rotating stall can and does occur in centrifugal compressors.

The propagation mechanism can be described by considering the blade row to be a cascade of blades (say, an inducer), as shown in Figure 30. A flow perturbation causes blade two to reach a stalled condition before the other blades. This stalled blade does not produce a sufficient pressure rise to maintain the flow around it, and an effective flow blockage or a zone of reduced flow develops. This retarded flow diverts the flow around it so that the angle of attack increases on blade three and decreases on blade one. The stall propagates downward relative to the blade row at a rate about half the blade speed; the diverted flow stalls the blades below the retarded-flow zone and unstalls the blades above it. The retarded flow or stall zone moves from the pressure side to the suction side of each blade in the opposite direction of rotor

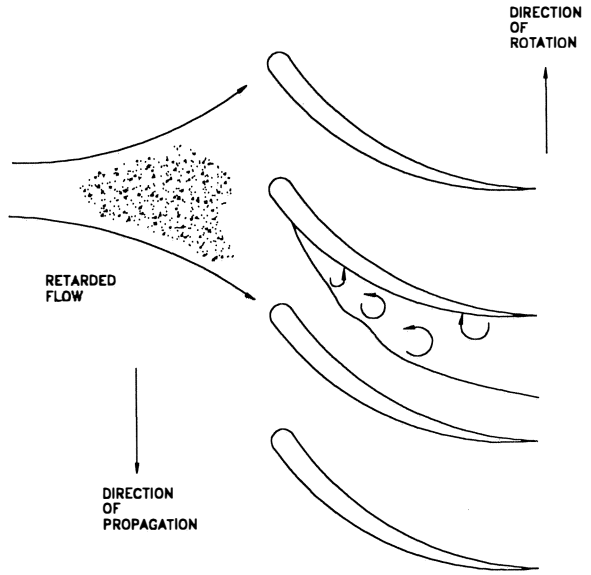

Figure 30. Rotating Stall in a Centrifugal Compressor Inducer.

rotation, and it may cover several blade passages. The relative speed of propagation has been observed from compressor tests to be less than the rotor speed (40 to 75 percent of rotor speed). Observed from an absolute frame of reference, the stall zones appear to be moving in the direction of rotor rotation. This phenomenon can lead to inefficient performance and excitation of the resonant frequency of the inducer, thus leading to failure of that section. Rotating stall is accompanied sometimes by a pulsating sound and pressure pulsations that can be noted at both the inlet and exit sections of the impellers.

Surge Detection and Control

Surge detection devices are those that attempt to avoid stall and surge by the measurement of some compressor parameters which meets or exceed the limit, of stable operation. A typical pressure oriented anti-surge control system is shown in Figure 31. The pressure transmitter monitors the pressure and controls a device which might open a blow-off valve. A temperature sensing device corrects the readings for the effect of flow and speed for the effect of temperature. A typical flow oriented surge control system is shown in Figure 32. These are two very simple surge control systems. More complex surge control systems are needed for complex configurations. With the advent of more computing power, surge lines can be adjusted automatically in the field to take care of operational changes.

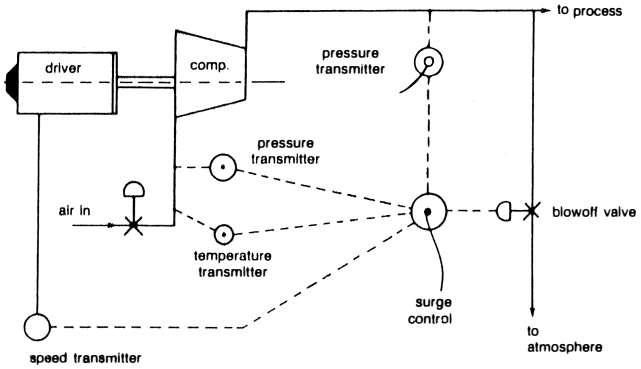

Figure 31. Pressure Oriented Anti-Surge Control System.

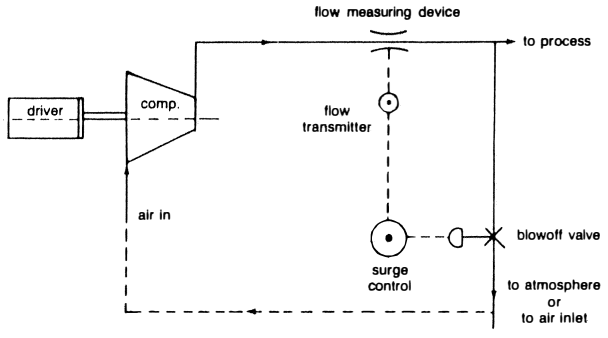

Figure 32. Flow Oriented Anti-Surge Control System.

Compressor Configuration

To properly design a centrifugal compressor, one must know the operating conditions—the type of gas, its pressure, temperature, and molecular weight. One must also know the corrosive properties of the gas so that proper metallurgical selection can be made. Gas fluctuations due to process instabilities must be pinpointed so that the compressor can operate without surging.

Centrifugal compressors for industrial applications have relatively low pressure ratios per stage. This condition is necessary so that the compressors can have a wide operating range while stress levels are kept at a minimum. Because of the low pressure ratios for each stage, a single machine may have a number of stages in one "barrel" to achieve the desired overall pressure ratio. Some of the many configurations are shown in Figure 33. Some factors to be considered when selecting a configuration to meet plant needs are:

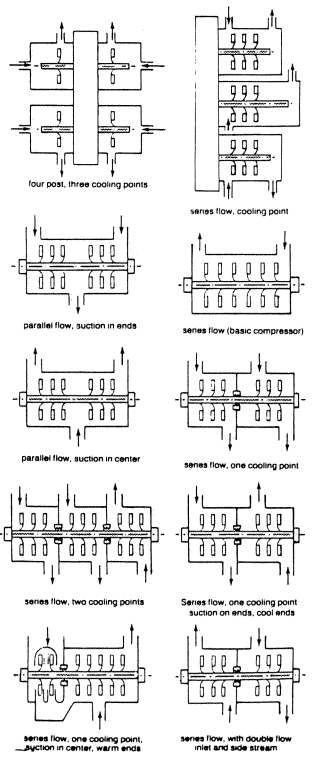

Figure 33. Various Configurations of Centrifugal Compressors.

- Intercooling between stages can considerably reduce the power consumed.
- Back-to-back impellers allow for a balanced rotor thrust and minimize overloading the thrust bearings.
- Cold inlet or hot discharge at the middle of the case reduces oil-seal and lubrication problems.
- Single inlet or single discharge reduces external piping problems.
- Balance planes that are easily accessible in the field can appreciably reduce field-balancing time.
- Balance piston with no external leakage will greatly reduce wear on the thrust bearings.
- Hot and cold sections of the case that are adjacent to each other will reduce thermal gradients, and thus reduce case distortion.
- Horizontally split casings are easier to open for inspection than vertically split ones, reducing maintenance time.
- Overhung rotors present an easier alignment problem because shaft end alignment is necessary only at the coupling between the compressor and driver.
- Smaller, high-pressure compressors that do the same job will reduce foundation problems, but will have greatly reduced operational range.

Impeller Fabrication

Centrifugal-compressor impellers are either shrouded or unshrouded. Open, shrouded impellers that are mainly used in single-stage applications are made by investment casting techniques or by three-dimensional milling. Such impellers are used, in most cases, for the high-pressure-ratio stages. The shrouded impeller is commonly used in the process compressor because of its low pressure ratio stages. The low tip stresses in this application make it a feasible design. Several fabrication techniques are shown in Figure 34. The most common type of construction is seen in (A) and (B) where the blades are fillet-welded to the hub and shroud. In (B), the welds are full penetration. The disadvantage in this type of construction is the obstruction of the aerodynamic passage. In (C), the blades are partially machined with the covers and then butt-welded down the middle. For backward lean-angled blades, this technique has not been very successful, and there has been difficulty in achieving a smooth contour around the leading edge. A slot-welding technique is illustrated in (D), and is used where blade-passage height is too small (or the backward lean-angle too high) to permit conventional fillet welding. In (E), an electron-beam technique is still in its infancy, and work needs to be done to perfect it. Its major disadvantage is that electron-beam welds should preferably be stressed in tension but, for the configuration of (E), they are in shear. The configuration of (G) through (J) use rivets. Where rivet heads protrude into the passage, aerodynamic performance is reduced. With today's technology in the area of welding, riveted impellers should be relegated to the scrap heap of history.

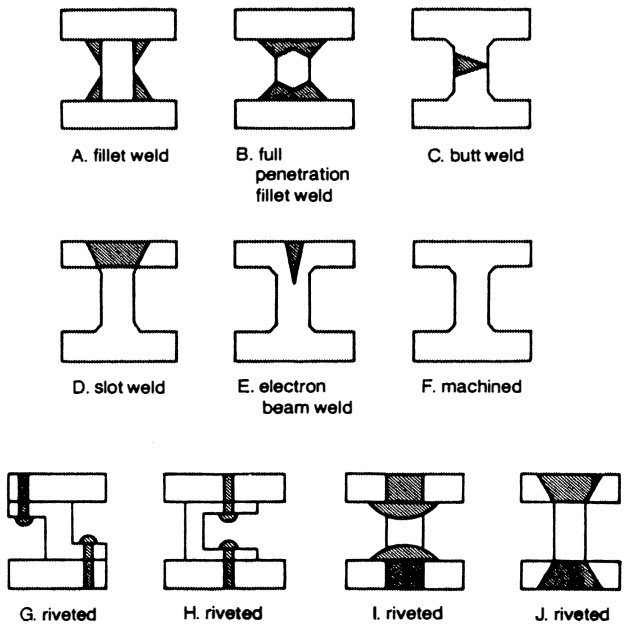

Figure 34. Several Fabrication Techniques for Centrifugal Impellers.

Materials for fabricating these impellers are usually low-alloy steels, such as AISI 4140 or AISI 4340. AISI 4140 is satisfactory for most applications; AISI 4340 is used for larger impellers requiring higher strengths. For corrosive gases, AISI 410 stainless steel (about 12 percent chromium) is used. Monel K-500 is employed in halogen gas atmospheres and oxygen compressors because of its resistance to sparking. Titanium impellers have been applied to chlorine service. Aluminum-alloy impellers have been used in great numbers, especially at lower temperatures (below 300°F). With new developments in aluminum alloys, this range is increasing. Aluminum and titanium are sometimes selected because of their low density. This low density can cause a shift in the critical speed of the rotor which may be advantageous.

BIBLIOGRAPHY

Alford, J. S., "Protecting Turbomachinery from Self-Excited Rotor Whirl," Journal of Engineering for Power, ASME Transaction, pp. 333-344 (October 1965).

Anderson, R. J., Riter, W. K., and Dilding, D. M., "An Investigation of the Effect of Blade Curvature on Centrifugal-Impeller Performance," NACA TN NO. 1313 (1947).

Balje, O. E., "A Contribution to the Problem of Designing Radial Turbomachines," ASME Trans., *74*, p. 451 (1952).

Balje, O. E., "A Study on Design Criteria and Matching of Turbomachines Part 13," *Journal of Engineering for Power*, ASME Trans., *84*, Series A, p. 103 (1962).

Balje, O. E., "A Study of Reynold Number Effects in Turbomachinery," Journal of Engineering for Power, ASME Trans. *86*, Series A, p. 227 (1964).

Balje, O. E., "Loss and Flow Path Studies on Centrifugal Compressors—Part I & II," ASME Paper No. 70-GT-12-A and 70-GT-12.B (1970).

Bammert, K. and Rautenberg, M., "On the Energy Transfer in Centrifugal Compressors," ASME Paper No. 74-GT-121 (1974).

Batman, J., "Design and Development of a Family of Natural Gas Compressors for a 3000 HP Gas Turbine Engine," ASME Paper No. 72-GT-10 (1970).

Benser, W. A. and Moser, J. J., "An Investigation of Back Flow Phenomena in Centrifugal Compressors," NACA Report No. 806 (1945).

Betz, A., *Introduction to the Theory of Flow Machines*, New York, New York: Pergamon Press (1966).

Bhinder, F. S. and Ingham, D. R., "The Effect of Inducer Shape on the Performance of High Pressure Ratio Centrifugal Compressors," ASME Paper No. 74-GT-122 (1974).

Boyce, M. P., "A Practical Three-Dimensional Flow Visualization Approach to the Complex Flow Characteristics in a Centrifugal Impeller," ASME Paper No. 66-GT-83 (1966).

Boyce, M. P. "Design of Compressor Blade Suitable for Transonic Axial-Flow Compressors," ASME Paper No. 76-GT-47 (1976).

Boyce, M. P., "How to Achieve Online Availability of Centrifugal Compressors," Chemical Engineering, pp. 115-117 (June 5, 1978).

Boyce, M. P., "Centrifugal Compressors," Process Equipment Series, *3* (1981).

Boyce, M. P., *Gas Turbine Engineering Handbook*, Houston, Texas: Gulf Publishing (1987).

Boyce, M. P. and Bale, Y. S., "Diffusion Loss in a Mixed Flow Compressor, Paper No. 729061, Intersociety Energy Conversion Compressor Impeller," NRCC ME-220, Ottawa, Canada, (July 1966).

Boyce, M. P. and Bale, Y. S., "A New Method for the Calculations of Blade Loadings in a Radial Flow Compressor," ASME Paper No. 71-GT-60 (1971).

Boyce, M. P. and Desai, A. R., "Clearance Loss in a Centrifugal Impeller," Paper No. 739126. Proc. of the 8th Intersociety Energy Conversion Engineering Conference, p. 638 (1973).

Boyce, M. P., Schiller, R. N. M., and Desai, A. R., "Study of Casing Treatment Effects in Axial Flow Compressors," ASME Paper No. 74-GT-89 (1974).

Boyce, M. P. and Hanawa, D. A., "Parametric Study of a Gas Turbine," *J. Eng. Power*, (December 1975).

Boyce, M. P., Morgan, E., and White, G., "Simulation of Rotor Dynamics of High Speed Rotating Machinery," Proceedings of

the First Int. Conf. Centrifugal Compressor Technol., pp. E6-32, Madras, India (1978).

Bullock, R. O. and Finger, H. B., "Surging in Centrifugal and Axial-Flow Compressors," SAE Quar. Trans. *6*, p. 220 (1952).

Cameron, J. A. and Danowski, F. M. "Some Metallurgical Considerations in Centrifugal Compressors," *Proceedings of the Second Turbomachinery Symposium*, The Turbomachinery Laboratory, The Texas A&M University System, College Station, Texas, pp. 116-128 (1973).

Campbell, K. and Talbert, J. E., "Some Advantages and Limitations of Centrifugal and Axial Compressors," SAE Trans., *53*, p. 607 (1945).

Cheshire, L. J., "Centrifugal Compressors for Aircraft Gas Turbines," Proc. L. Mech. E., *153*, 1965; reprinted by the ASME, "Lectures on the Development of the British Gas-Turbine Jet Unit" (1967).

Clapp, A. M., "Fundamentals of Lubrications Relating to Operation and Maintenance of Turbomachinery," *Proceedings of the First Turbomachinery Symposium*, The Turbomachinery Laboratory, The Texas A&M University System, College Station, Texas, pp. 66-74 (1972).

Concorida, C. and Dowell, M. F., "Analytical Design of Centrifugal Air Compressors," J. App. Mechs., *13*, p. A-271 (1946).

Coppage, J. E., et al., "Study of Supersonic Radial Compressors for Refrigeration and Pressurization System," WADC Technical Report 55-257, Astia Document No. AD 110467 (1956).

Curle, N. and Skan, S. W., "Approximate Method for Predicting Separation Properties of Laminar Boundary Layers," Aero Wuart, G, 257 (August 1957).

Davis, H. M., Centrifugal Compressor Operation and Maintenance, *Proceedings of the First Turbomachinery Symposium,* The Turbomachinery Laboratory, The Texas A&M University System, College Station, Texas, pp. 10-25 (1972).

Dean, R. C., "The Fluid Dynamic Design of Advanced Centrifugal Compressors," Von Karman Institute, Lecture Notes No. 50, (1972).

Delamey, R. A. and Kavanagh, P., "Transonic Flow Analysis in Axial Flow Turbomachinery Cascades by a Time-Dependent Method of Characteristics," ASME Paper No. 75-GT-8 (1975).

Eckardt, D., "Instantaneous Measurements in the Jet-Wake Discharge Flow of a Centrifugal Compressor Impeller," ASME Paper No. 74-GT-90 (1974).

Eckert, B., "Axial and Radialkompressoren," Springer (1953).

Edminister, W. C., *Applied Hydrocarbon Thermodynamics*, Houston, Texas: Gulf Publishing (1983).

Ehrich, F. F., "Identification and Avoidance of Instabilities and Self-Excited Vibrations in Rotating Machinery," Adopted from ASME Paper 72-DE-21. General Electric Co., Aircraft Engine Group, Group Engineering Division, (1972).

Ellis, G. D. and Stanitz, J. D., "Two Dimensional Compressible Flow in Centrifugal Compressors with Logarithmic-Spiral Blades, NACA TN No. 2255 (1951).

Ellis, G. O. and Stanitz, J. D., "Comparison of Two and Three-Dimensional Potential-Flow Solutions in a Rotating Impeller Passage," NACA TN No. 2806 (1952).

Ferguson, T. B., "The Centrifugal Compressor Stage," Butterworth and Co., Ltd., London (1963).

Flaherty, R., "A Method for Estimating Turbulent Boundary Layers and Heat Transfer in an Arbitrary Pressure Gradient," United Aircraft Research Laboratories Report UAR-G51 (August 1968).

Fowler, H. S., "An Investigation of the Flow Processes in a Centrifugal Compressor Impeller," NRCC ME-220, Ottawa, Canada (July 1966).

Fowler, H. S., "Experiments on the Flow Processes in Simple Rotating Channels," NRCC ME-229, Ottawa, Canada (1969).

Ginsberg, A., Ritter, W. K., and Polasics, J., "Effects of Performance of Changing the Division of Work Between Increase of Angular Velocity and Increase of Radius of Rotation in an Impeller," NACA TN No. 1216 (1947).

Gregory, A. T., "Elastic Fluid Compressor," United States Patent Office, 3305165 (February 21, 1967).

Gresh, M. T., "Compressor Performance," Butterworth and Heinemann (1991).

Gunter, E. J., "Dynamic Stability of Rotor Bearing Systems," NASA Sp-113 (1966).

Gunter, E. J., Jr., "Rotor Bearing Stability," *Proceedings of the First Turbomachinery Symposium*, The Turbomachinery Laboratory, The Texas A&M University System, College Station, Texas (1972).

Haag, A. C., "The Influences of Oil Film Journal Bearings on the Stability of Rotating Machines," J. of Appl. Mech. Trans. ASME, *68*, p. 211 (1946).

Hamrick, J. T., Ginsbert, A., and Osborn, W. M., "Method of Analysis for Compressible Flow Through Mixed-Flow Centrifugal Impellers of Arbitrary Design," NACA Report No. 1082 (1952).

Hansen, A. G. (Editor), "Symposium on Fully Separated Flows," ASME Fluids Energy Division Conference, Philadelphia, Pennsylvania (1964).

Hayes, W. D., "The Three Dimensional Boundary Layer" NAVORD Report No. 1313, Washington, D.C., 1051.

Herbage, B. S., "High Speed Journal and Thrust Bearing Design," *Proceedings of the First Turbomachinery Symposium,* The Turbomachinery Laboratory, The Texas A&M University System, College Station, Texas, pp. 55-61 (1972).

Housmann, J. G., "Turbomachinery Specifications," *Proceedings of the First Turbomachinery Symposium*, The Turbomachinery Laboratory, The Texas A&M University System, College Station, Texas, pp. 77-78, (1972).

Jackson, C. J., "Cold and Hot Alignment Techniques for Turbomachinery," *Proceedings of the Second Turbomachinery Symposium*, The Turbomachinery Laboratory, The Texas A&M University System, College Station, Texas, pp. 1-7 (1973).

Kasai, T., "On the Exit Velocity and Slip Coefficient of Flow at the Outlet of the Centrifugal Pump Impeller," Memoirs of the Faculty of Engineering, Kyushu Imperial University, Japan, *8*, (1) (1936).

Katsanis, T., "Use of Arbitrary Quasi-Orthogonals for Calculating Flow Distribution in the Meridional Plane of a Turbomachine," NASA TND-2546 (1964).

Kearton, W. F., "The Influence of the Number of Impeller Blades on the Pressure Generated in a Centrifugal Compressor and of its General Performance," Proc. I. Mech. E., *124*, p. 481 (1933).

Klassen, H. A., "Effect of Inducer Inlet and Diffuser Throat Areas on Performance of a Low Pressure Ratio Sweptback Centrifugal Compressor," NASA TM X-3148, Lewis Research Center (January 1975).

Kovats, A., "Design and Performance of Centrifugal and Axial Flow Pumps and Compressors," New York, New York: The Macmillan Co. (1964).

Kramer, J. J., Osborn, W. M., and Hamrick, J. T., "Design and Test of Mixed-Flow and Centrifugal Impellers," *Journal of Engineering for Power*, ASME Trans., Series A., *82*, p. 127 (1960).

Kuethe, A. M. and Schetzer, J. D., *Foundations of Aerodynamics*, New York, New York: John Wiley & Sons (1950).

Lapina, R. P., *Estimating Centrifugal Compressor Performance*, Houston, Texas: Gulf Publishing (1981).

Lazarkiewicz, S. and Troskolanski, A. T., "Impeller Pumps," Pergamon Press (1965).

Lesiecki, G., "Evaluation of Liquid Film Seals: Associated Systems and Process Considerations," *Proceedings of the Sixth*

Turbomachinery Symposium, The Turbomachinery Laboratory, The Texas A&M University System, College Station, Texas, pp. 145-148 (1977).

Lewis, R. A., "Mechanical Contact Shaft Seal," *Proceedings of the Sixth Turbomachinery Symposium,* The Turbomachinery Laboratory, The Texas A&M University System, College Station, Texas, 1977.

Lown, H. and Wiesner, F. J., Jr., "Prediction of Choking Flow in Centrifugal Impeller," Transaction of ASME Journal of Basic Engineering, (March 1959).

Mechanical Engineers Handbook, "Centrifugal and Axial Fans," 6th Edition, p. 14-66 to 14-79.

Michel, D. J., Mizisin, J., and Prian, V. D., "Effect of Changing Passage Configuration on Internal-flow Characteristics of a 48-inch Centrifugal Compressor," NACA TN No. 2706 (1952).

Mikolajczak, A. A., Weingold, H. D., and Nikkanen, J. P., "Flow Through Cascades of Slotted Compressor Blades," Journal of Engineering for Power, ASME Trans., p. 57 (January 1970).

Moody, L.F., "Friction Factors," ASME Trans., p. 672, (November 1944).

Newkirk, B. L., "Shaft Whipping," General Electric Review, *27*, p. 169 (1924).

Nuell, W. V. D., "The Maximum Delivery Pressure of Single Stage Radial Supercharges for Aircraft Engines," NACA TN No. 949 (1940).

Owczarek, J. A., *Fundamentals of Gas Dynamics*," Philadelphia, Pennsylvania: International Textbook Company (1968).

Peck, J. F., "Investigations Concerning Flow Conditions in a Centrifugal Pump, and the Effect of Blade Loading of Head Slip," Proc. I. Mech. E., *164*, (1), p. 1 (1951).

Petermann, H., Untersuchungen a m Zentsipetalrad fur Kreiselverdichter Forshung, *17* (1952).

Pfleiderer, C., "Kreisel pumpen," Springer, F155.

Prian, V. D. and Michel, D. J., "An Analysis of Flow in Rotating Passage of Large Radial Inlet Centrifugal Compressor at Top Speed of 700 Feet Persecond," NACA TN No. 2584 (1951).

Reshotko, E. and Tucker, M., "Approximate Calculation of the Compressible Turbulent Boundary Layer with Heat Transfer and Arbitrary Pressure Gradient," NACA Tn 4154 (1954).

Ribary, F., "The Friction Losses of Steam Turbine Discs," Brown Boveri Review, *21*, p. 120 (1934).

Ritter, W. K. and Johnson I. A., "Performance Effect of Fully Shrouded a Centrifugal Supercharger Impeller," NACA ARR E5H23 or E18.

Rodgers, C., "Influence of Impeller and Diffuser Characteristics and Matching on Radial Compressor Performance," SAE Reprint 268B (January 1961).

Rodgers, C., "Typical Performance Characteristics of Gas Turbine Radial Compressors," *Journal of Engineering for Power*, ASME Trans., p. 161 (April 1964).

Rodgers, C. and Sapiro, L., "Design Considerations for High Pressure Ratio Centrifugal Compressors," ASME Paper No. 72-GT-91 (1972).

Sawyer's Gas Turbine Engineering Handbook—Vol. I, II, III.

Sapiro, L., "Preliminary Staging Selection for Gas Turbine Driven Centrifugal Gas Compressors," ASME Paper No. 73-GT-31 (1973).

Schlichting, H., "Application of Boundary-Layer Theory in Turbomachinery," ASME Trans. *81*, p. 543 (1959).

Schlichting, H., *Boundary Layer Theory*, New York, New York: McGraw-Hill Book Co. (1968).

Schmieden, C., "Uber den Widerstand einer in einer Flussigkeit Rotierenden Scheibe," ZAMM *8*, p. 460 (1928).

Schultz-Grunow, F., "Der Eirbungswiderstand Rotierender Scheiben in Gehansen" ZAMM *15*, p. 191 (1935).

Senoo, Y. and Nakase, Y., "An Analysis of Flow Through a Mixed Flow Impeller," ASME Paper No. 71-GT-2 (1971).

Senoo, Y., et al., "Viscous Effects on Slip Factor of Centrifugal Blowers," ASME publication 73-GT-56 (1973).

Sheets, H. E., "The Flow Through Centrifugal Compressors and Pumps," ASME Trans. *72*, p. 1009 (1950).

Shepherd, D.G., *Principles of Turbomachinery*, New York, New York: The MacMillan Company, (1957).

Shouman, A. R. and Anderson, J. R., "The Use of Compressor Inlet Prewhirl for the Control of Small Gas Turbines," Journal of Engineering for Power, Trans. ASME Ser. A., *86*, pp. 136-140 (1964).

Sovran, G. and Klomp, E. D., *Fluid Mechanics of Internal Flow*, New York, New York: Elsevier Publishing Co. (1967).

Speer, I. E., "Design and Development of a Broad Range High Efficiency Centrifugal Compressor for a Small Gas Turbine Compressor Unit, ASME Paper No. 52-SA-14 (1952).

Stahler, A. F., "Transonic Flow Problems in Centrifugal Compressors," SAE Reprint 268C (January 1961).

Stanitz, J. D., "Two Dimensional Compressible Flow in Conical Mixed Flow Compressors," NACA TN No. 1744 (1948).

Stanitz, J. D., "Two Dimensional Compressible Flow in Turbomachines with Conic Flow Surfaces," NACA Report No. 935 (1949).

Stanitz, J. D., "Some Theoretical Aerodynamic Investigation of Impellers in Radial and Mixed Flow Centrifugal Compressors," ASME Trans. *74*, p. 472 (1952).

Stanitz, J. D. and Ellis, G. O., "Two Dimensional Compressible Flow In Centrifugal Compressors with Straight Blades," NACA Report No. 954 (1950).

Stanitz, , J. D. and Ellis, G. O., "Two Dimensional Flow on General Surfaces of Revolution in Turbomachines," NACA TN 2654.

Stanitz, J. D. and Brian, V. D., "A Rapid Approximate Method for Determining Velocity Distribution on Impeller Blades of Centrifugal Compressors," NACA TN No. 2421 (1951).

Stepanoff, A.J., Turboblowers, New York, New York: Wiley (1955).

Stepanoff, A. J., *Centrifugal and Axial Flow Pumps*, New York, New York: John Wiley & Sons, Inc., (1968).

Stockman, N. O. and Kramer, J. L., "Method for Design of Pump Impellers Using a High Speed Digital Computer," NASA TND 1562.

Stodola, A., "Steam and Gas Turbines," New York, New York: Mc-Graw-Hill Book Co., (1927).

Thomson, W. T., *Mechanical Vibrations*, Second Edition, Englewood Cliffs, New Jersey: Prentice-Hall, Inc. (1961).

Vavra, M. H., *Aerothermodynamics and Flow in Turbomachines*, New York, New York: John Wiley & Sons, Inc. (1960).

Watabe, K., "Effects of Clearances and Grooves on Fluid Friction of Rotation Discs," JSME Bulletin, *8*, (29), p. 55 (February 1965).

Watabe, K., JSME Bulletin, *7*, (November 26, 1966).

Watabe, K., "Experiments on Fluid Friction of Rotating Disc with Blades," Japan Society of Mechanical Engineers Bulletin, *5*, (17).

Wiesner, F. J., Jr., "Practical Stage Performance Correlations for Centrifugal Compressors," ASME Paper No. 60-Hyd-17 (1960).

Wilcock, D. E. S. and Booser, E. R., "Bearing Design and Application," New York, New York: McGraw-Hill (1961).

Wislicensu, G. F., "Fluid Mechanics of Turbomachinery," New York, New York: Mc-Graw-Hill Book Co., Inc. (1947).

Woodhouse, H., "Inlet Conditions of Centrifugal Compressors for Aircraft Engine Superchargers and Gas Turbines," J. Inst. Aeron. Sc., *15*, p. 403 (1948).

Wu, C. H., "A General Theory of Three Dimensional Flow in Subsonic and Supersonic Turbomachines of Axial, Radial and Mixed-Flow Type," NACA TN 2604, (1952).

Yuan, S.W., *Foundations of Fluid Mechanics*, New Delhi, India: Prentice Hall (1969).

York, R. E. and Woodard, H. S., "Supersonic Compressor Cascades—An Analysis of the Entrance Region Flow Field Containing Detached Shock Waves," ASME Paper No. 75-GT-33 (1975).